Post-liquefaction Reconsolidation and Undrained Cyclic Behaviour of Chang Dam Soil

Majid Hussain and Ajanta Sachan

Abstract Understanding and determination of post-liquefaction stress–strain behavior of sandy soils under monotonic and cyclic loading is essential to estimate the deformations that might occur in liquefied deposits under further loading. The undrained response of reconsolidated specimens under multilevel cyclic loading simulates the post-liquefaction behavior of soils under earthquake aftershocks and other cyclic loading conditions. In the present study, post-liquefaction reconsolidation and undrained behavior of medium dense silty-sand of Chang dam under multilevel repeated cyclic loading is explored. The soil deposit underwent severe liquefaction during the 2001 Bhuj earthquake. During the first round of loading (C_0), the specimens were subjected to 50 cycles of cyclic loading at 0.4 mm amplitude (A) and 0.1 Hz frequency (f) and exhibited liquefaction. After C_0, developed excess pore water pressure was allowed to dissipate, and specimens were allowed to reconsolidate. Reconsolidated specimens were then subjected to second round of cyclic loading, C_1 ($A = 0.4$ mm, $f = 0.1$ Hz and $N = 35$), and this process was continued for C_2, C_3, and C_4 loading rounds. Significant reduction in void ratio (e) was observed each time when specimens were allowed to reconsolidate after each round of undrained cyclic loading, thereby increasing the liquefaction resistance. The increase in liquefaction resistance on repeated loading was reflected in the cyclic stress ratio (CSR) calculated for every cycle for each level of cyclic applied loading. The inclination of the peak deviatoric stress envelope (instability line) for each round of loading was observed to increase with repeated reconsolidation and cyclic loading.

Keywords Post-liquefaction · Cyclic loading · Reconsolidation · Stress path · Cyclic stress ratio (CSR)

M. Hussain (✉) · A. Sachan
Indian Institute of Technology Gandhinagar, Gandhinagar, India
e-mail: majid.hussain@iitgn.ac.in

A. Sachan
e-mail: ajanta@iitgn.ac.in

A. Prashant et al. (eds.), *Advances in Computer Methods and Geomechanics*, Lecture Notes in Civil Engineering 55,
https://doi.org/10.1007/978-981-15-0886-8_7

1 Introduction

When loose saturated sand deposits are subjected to shaking during an earthquake, there is reduction of mean effective stress (p') due to the buildup of excess pore water pressure (Δu) subsequently leading to liquefaction under undrained boundary conditions. Understanding the phenomenon of liquefaction and the methods to mitigate its effects has received considerable attention for the past few decades. The post-liquefaction mechanical behavior of soils is as important as liquefaction. Awareness about the post-liquefaction reconsolidation and stress–strain behavior of soils susceptible to liquefaction is necessary to estimate the earthquake-induced settlements and to evaluate the bearing capacity of the liquefied soil deposits [7, 27]. The effect of previous seismic stress–strain history (cyclic pre-shearing) is important in evaluating the undrained response of liquefied soil deposits. In addition to the induced shear strains (γ), pore pressure (Δu) and degree of post-liquefaction reconsolidation, undrained mechanical behavior of liquefied soils deposits is governed by the same factors that govern the liquefaction behavior of soils, viz, density, fines content, nature of fines, mode of loading, initial effective consolidation pressure (p'_c), and loading history. Initially, till early 1990s minimal work was carried out to understand the post-liquefaction behavior of sands [5, 24]. However, more recently various researchers [4, 10, 15, 17, 18, 23, 25] studied the post-liquefaction undrained shear behavior of sandy soils. Olson and Stark [12, 13] suggested a detailed procedure based on a well-documented large database of case histories to evaluate the liquefied strength and post-liquefaction stability of soil deposits susceptible to liquefaction.

Earthquake-induced ground settlements have two components: one resulting during the process of shear deformation of the soil (liquefaction) and the other due to reconsolidation of the liquefied deposits. Settlements resulting from post-liquefaction reconsolidation were reported to be directly related to the maximum induced γ and Δu; which developed during liquefaction [8]. A strong relationship between the post-liquefaction volumetric strains and the factor of safety against liquefaction was reported. Post-liquefaction reconsolidation behavior of the liquefied saturated sandy soils was explored by analyzing pore pressure dissipation curves using solidification and consolidation theory [20, 21]. The increased permeability after liquefaction (~5 times of the initial value) was also observed to facilitate larger settlements during reconsolidation stage of the liquefied deposits [3].

The post-liquefaction undrained monotonic shear behavior of liquefied soils was reported by many researchers [2, 4, 15, 17, 18, 24, 25]. If excess pore water pressure at the end of cyclic loading was allowed to dissipate, the post-liquefaction undrained monotonic stress–strain response was observed to be strongly dependent on relative density including the insignificant influence of amplitude of axial strain and initial confining pressure [18]. Amini and Trandafir [2] reported that the liquefied soil deposits would exhibit dilative post-liquefaction shear strength response, which would be strongly dependent on initial effective consolidation stress (p'_c). Wang et al. [26] observed that post-liquefaction shear strength and stiffness increased with the increase in the degree of reconsolidation both at small and large deformations. The

mentioned research also studied the post-liquefaction undrained monotonic behavior of soils considering the effect of degree of reconsolidation, relative density, initial effective confining pressure (p'_c), fines content, nature of fines, and shear strain amplitude. Robertson [16] presented cone penetration test (CPT)-based relationships to evaluate liquefied shear strength for a wide range of soils based on well-documented case histories. The case histories indicated that young, loose, nonplastic, or low-plastic soils would tend to be more susceptible to significant and rapid strength loss than older, denser and more plastic soils.

A number of investigators also explored liquefaction characteristics of previously liquefied soils under triaxial or simple shear testing conditions [5, 9]. The studies confirmed that liquefaction resistance of previously liquefied specimen could exhibit a marked increase or decrease in its response depending on the level of induced shear strain (γ), excess pore water pressure (Δu), and the initial relative density (D_r) of the specimens. It might be due to the elimination of local instabilities and creation of a nonuniform structure [5]. Oda et al. [14] provided microstructural interpretation of liquefaction mechanism of liquefied granular soils under cyclic loading. Influence of cyclic pre-shearing on undrained cyclic behavior of cohesionless soils was studied by Porcino et al. [15] and Sriskandakumar et al. [17]. The findings revealed that the cyclic response of pre-sheared specimens would depend on the degree of Δu and level of γ reached during the previous cyclic loading. Current study is focused on the evaluation of reconsolidation and liquefaction response of previously liquefied silty-sand specimens under multilevel undrained cyclic triaxial conditions. The research work was carried out to understand the reconsolidation and liquefaction response of already liquefied specimens to simulate the behavior under earthquake aftershocks and other cyclic loading conditions in high seismicity region. The response of reconsolidated specimens under four levels of cyclic loading after initial liquefaction was explored. The material studied consists of medium dense silty-sand collected from Chang dam of Kucth region Gujarat, India. The soil had experienced severe liquefaction during the 2001 Bhuj earthquake resulting in significant damage to the dam [19].

2 Experimental Program

2.1 Material Properties and Specimen Preparation

In the present study, the soil was collected from downstream toe of Chang dam at a depth of 0.5 m. The soil consists of 82% sand, 15% silt, and 1% clay and classified as medium dense silty-sand (SM). Basic geotechnical properties of the Chang dam soil are presented in Table 1. The grain size distribution (GSD) of the soil is illustrated in Fig. 1. Solid cylindrical specimens of 50 mm diameter and 100 mm height were prepared using moist tamping method at in situ dry density and water content of 1.6 g/cm^3 and 8%, respectively.

Table 1 Basic properties of test material

D_{10}	D_{50}	C_u	C_c	G_S	e_{max}	e_{min}	FC	*Soil class*
0.02	0.19	10	4.225	2.66	0.851	0.496	18	SM

where D_{10} and D_{50} are effective and mean particle diameters in mm, C_u and C_c are coefficients of uniformity and curvatures, respectively, G_S specific gravity, e_{max} and e_{min} are maximum and minimum void ratio and FC is fines content in %

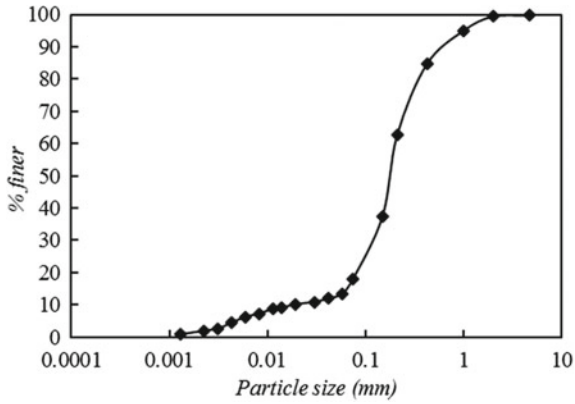

Fig. 1 Grain size distribution of Chang dam soil

2.2 Testing Procedure

The post-liquefaction reconsolidation and undrained cyclic behavior of medium dense silty-sand of Chang dam was investigated by conducting a series of isotropically consolidated undrained cyclic triaxial tests under strain-controlled conditions. In post cyclic loading, the liquefied specimens were subjects to four rounds of reconsolidation and undrained cyclic loading to evaluate the post-liquefaction cyclic behavior of the specimens. A schematic representation of the testing procedure along with drainage conditions is mentioned in Fig. 2. The prepared soil specimens were mounted on the loading frame of cyclic cum static triaxial testing machine and were saturated in three steps: CO_2 saturation, water flushing, and back pressure saturation. Specimens were flushed with CO_2 for 45 min at very low pressure (~5 kPa) while maintaining a cell pressure of 20 kPa [11]. After CO_2 flushing, water flushing was conducted by pushing water inside the specimen equal to 2–3 times the volume of the specimen. Back pressure was then applied in increments of 40 kPa (every 2 h) to acquire B (Skempton's pore pressure parameter) values greater than 0.98. During the saturation stage, the effective confining stress (p') was maintained at 20 kPa. After saturation, the specimens were isotropically consolidated to respective effective confining pressure (p'_c) of 100, 200, and 300 kPa. The consolidated specimens were further subjected to first round (C_0) of undrained (constant volume) harmonically varying cyclic axial loading of amplitude (A) 0.4 mm and frequency (f) 0.1 Hz

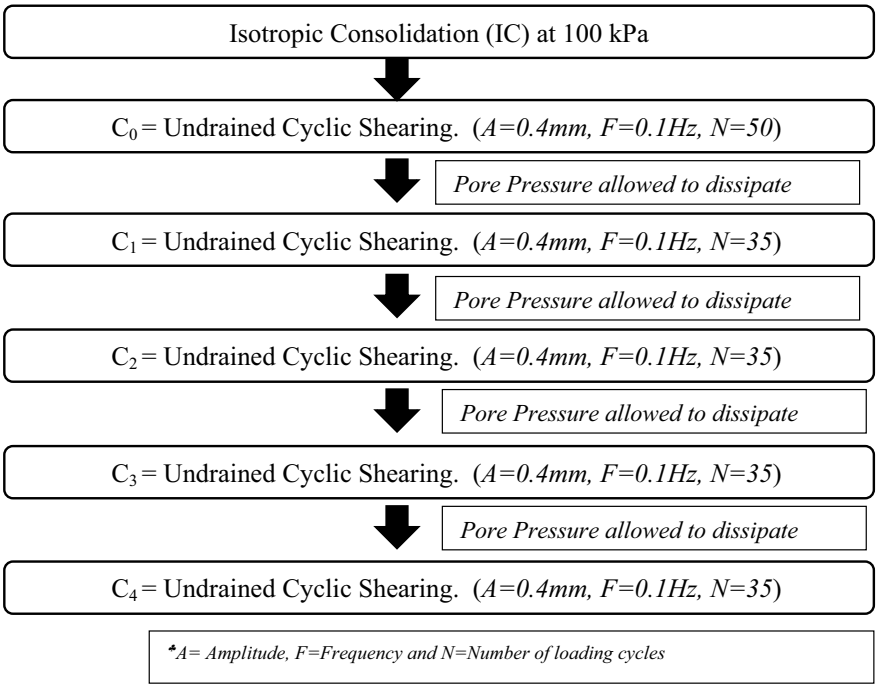

Fig. 2 Procedure adopted for repeated multilevel reconsolidation and cyclic loading

for 50 number of cycles (N). The liquefied specimens were then allowed to reconsolidate and further subjected to second round (C_1) of cyclic loading, ($A = 0.4$ mm, $f = 0.1$ Hz, and $N = 35$). The process was repeated three more times to arrive at the fourth round (C_4) of cyclic loading, as shown in Fig. 2. The number of cycles was restricted to 50 and 35 as the specimens exhibited liquefaction within 10 cycles during C_0.

3 Results and Discussion

Loose silty-sands are most susceptible to liquefaction owing to the large compressibility and small-undrained shear strength. These soils undersaturated and undrained conditions undergo liquefaction, even under moderate seismic/earthquake events. Due to their large susceptibility to liquefaction, the post-liquefaction cyclic behavior of such soils becomes essential to evaluate the settlements that will result from reconsolidation and further cyclic loading (aftershocks and other cyclic loads). The current study evaluates the cyclic, post-liquefaction reconsolidation, and undrained behavior of medium dense silty-sand of Chang dam under multilevel cyclic loading.

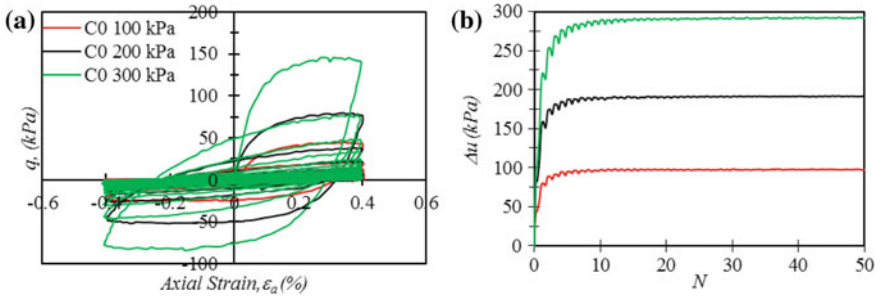

Fig. 3 Response of Chang dam soil during C_0. **a** Stress–strain, **b** excess pore water pressure

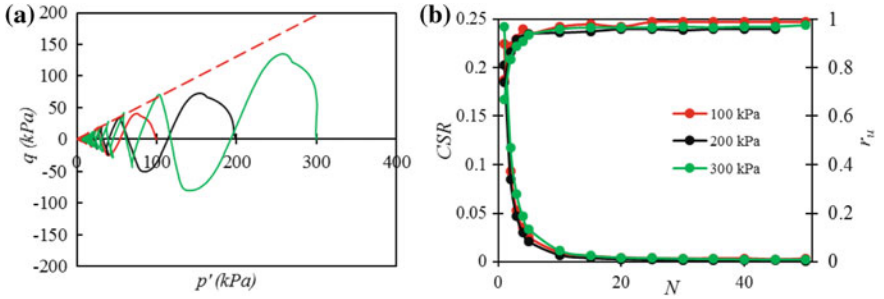

Fig. 4 Response of Chang dam soil during C_0. **a** Effective stress path, **b** evolution of *CSR* and r_u

Chang soil exhibited low liquefaction resistance under first round (C_0) of the applied strain control loading of amplitude (A) and frequency (f) to be 0.4 mm and 0.1 Hz, respectively. Figure 3 illustrates the stress–strain and excess pore water pressure (Δu) response of the soil at the three initial confining pressures (p'_c) of 100, 200, and 300 kPa. The specimens exhibited initial liquefaction within five cycles with Δu attaining values nearly equal to initial confining pressure (p'_c). Figure 4 shows the effective stress path and evolution of cyclic stress ratio (*CSR*) and excess pore water pressure ratio (r_u) with the number of loading cycles (N) for the specimens at the three p'_c. It was observed that *CSR* exhibited values as low as 0.003 at N equal to 10. The corresponding r_u values were evaluated to be higher than 0.97, indicating nearly initial liquefaction (Fig. 3b).

3.1 Post-Liquefaction Reconsolidation Behavior Under Repeated Multilevel Cyclic Loading

After C_0, the developed Δu was allowed to dissipate (reconsolidation) resulting in decreased void ratio. Subsequent cyclic loading after each level (round) is illustrated

Table 2 Reduction in void ratio during reconsolidation after each level of cyclic loading

p_c' kPa	Δe				
	IC	C_0	C_1	C_2	C_3
100	0.035	0.038	0.022	0.016	0.012
200	0.042	0.043	0.026	0.017	0.013
300	0.048	0.053	0.032	0.022	0.017

in Fig. 2. Reduction in void ratios due to reconsolidation at the end of four rounds of cyclic loading are presented in Table 2. The specimens exhibited significant decrease in void ratios with the increase in p'_c and with the subsequent levels of cyclic loading. The decrease in void ratio during reconsolidation after a particular round of loading was observed to increase with p'_c. At given p'_c, the reduction in void ratio decreased with the subsequent rounds of cyclic loading (Δe during reconsolidation decreased as the loading progressed from level C_0 to C_3), as mentioned in Table 2. The reduced void ratio led to lower compressibility, which resulted in suppressed contractive behavior and increased resistance to liquefaction on subsequent repeated cyclic loading. The reconsolidation volumetric strains could be directly transformed to the maximum shear strain amplitudes that might result during a seismic event [8].

3.2 Post-liquefaction Undrained Stress–Strain and Pore Pressure Behavior Under Repeated Multilevel Cyclic Loading

Specimens reconsolidated after C_0 was subjected to the second round (C_1) of cyclic loading (A = 0.4 mm and $f = 0.1$ Hz for N = 35). Figure 5a illustrates the response of specimens subjected to C_1. During C_1, q_{max} for each cycle was observed to be higher as compared to C_0 except for the first cycle. The lower value of q_{max} during first cycle might be due to the weakening of the soil fabric resulting from excessively high levels of r_u [17]. Although the immediate peak deviatoric stress was observed to be lower as compared to C_0, the reconsolidated specimens exhibited higher liquefaction resistance to further cyclic loading. This could be attributed due to the reduced void ratio resulting in more compact packing of the soil particles. Evolution of *CSR* and r_u with number of loading cycles (N) exhibited continuous decrease and increase, respectively for both C_0 and C_1. However, the respective values for C_1 were lower for r_u and higher for *CSR* as compared to C_0. Peak parameters evaluated at the end of loading cycles 1, 5, 10, and 35 are presented in Table 3.

After C_1, the specimens were allowed to reconsolidate and further subjected to C_2. Figure 5b illustrates the stress–strain and pore pressure response of the soil specimens subjected to C_2. Both *CSR* and r_u evolved at a slower rate during C_2 as compared to C_1 and C_0. The specimens exhibited significant improvement in liquefaction resistance

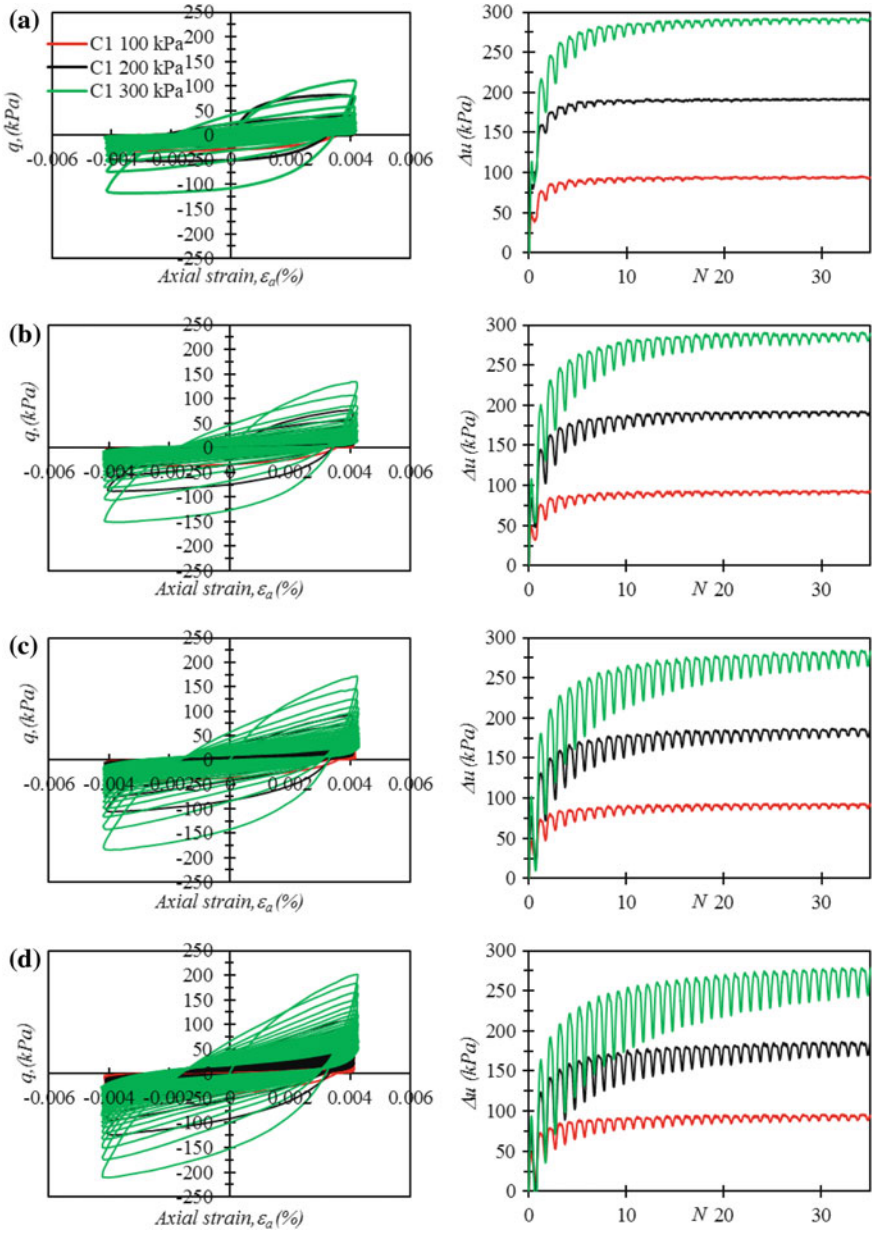

Fig. 5 Stress–strain behavior (**A**) and pore pressure response (**B**) of Chang dam soil subjected to repeated multilevel cyclic loading. **a** C_1, **b** C_2, **c** C_3, **d** C_4

Table 3 Summary of the test results of repeated multilevel reconsolidation and cyclic loading

p'_c	100 kPa				200 kPa				300 kPa			
N	1	5	10	35	1	5	10	35	1	5	10	35
C_0												
q_{max}	43.0	7.2	3.6	1.5	81.0	8.3	2.7	0.6	145.5	24.6	9.7	2.7
r_u	0.76	0.96	0.98	0.99	0.75	0.94	0.96	0.97	0.69	0.95	0.98	0.99
CSR	0.215	0.036	0.018	0.007	0.203	0.021	0.007	0.002	0.243	0.041	0.016	0.004
C_1												
q_{max}	31.2	7.4	4.7	2.1	81.7	11.5	4.5	1.5	111.4	37.2	19.0	5.7
r_u	0.71	0.96	0.96	0.97	0.74	0.94	0.95	0.96	0.62	0.90	0.95	0.97
CSR	0.156	0.037	0.024	0.011	0.204	0.029	0.011	0.004	0.186	0.062	0.032	0.009
C_2												
q_{max}	36.0	11.8	8.1	3.7	76.8	30.4	17.3	7.4	134.4	62.3	37.1	13.8
r_u	0.70	0.95	0.96	0.98	0.61	0.89	0.93	0.96	0.53	0.86	0.93	0.97
CSR	0.18	0.059	0.041	0.018	0.192	0.076	0.043	0.018	0.224	0.104	0.062	0.023
C_3												
q_{max}	41.2	15.2	11.4	5.4	91.8	44.2	27.8	11.1	172.1	98.2	66.1	27.8
r_u	0.64	0.92	0.92	0.94	0.52	0.84	0.89	0.93	0.43	0.79	0.88	0.95
CSR	0.21	0.076	0.057	0.027	0.229	0.111	0.070	0.028	0.287	0.164	0.110	0.046
C_4												
q_{max}	45.4	19.7	14.7	6.6	111.0	60.9	41.3	18.5	201.6	138.5	102.5	51.26
r_u	0.57	0.89	0.89	0.93	0.45	0.80	0.87	0.93	0.33	0.74	0.83	0.93
CSR	0.227	0.10	0.074	0.03	0.278	0.152	0.103	0.046	0.336	0.231	0.171	0.085

and were reflected in *CSR* and r_u evaluated at the end of cycles 1, 5, 10, and 35 (Table 3).

After C_2, specimens were subjected to two more rounds of reconsolidation and cyclic loading (C_3 and C_4). Figures 5c, d illustrate the stress–strain and pore pressure response of Chang dam soil subjected to C_3 and C_4. The results indicated further increase in liquefaction resistance as compared to previous round of cyclic loading. This was reflected in the increasing *CSR* and decreasing r_u for each cycle of subsequent loading rounds, as mentioned in Table 3. The r_u at the end of a particular cycle was found to be lower in subsequent levels of cyclic loading. A significant increase in deviatoric stress as compared to r_u was observed under repeated cyclic loading. This could be attributed due to the reduced void ratio thereby shifting the state of soil specimens lower and closer to the critical state line (*CSL*). The closeness of the state of specimen to the *CSL* increased upon subsequent levels of loading and hence the higher deviatoric stress was observed. This effect was found to increase with the increasing p'_c. For C_4 and p'_c equal to 300 kPa, $q_{\max}$ and p' at the end of 35 cycles were evaluated to be 51.3 kPa and 25 kPa, respectively, which indicated the strength degradation rather than initial liquefaction. Stress–strain response of specimens showed increased stiffness as compared to previous loading round (Fig. 5). During C_4, *CSR* at the end of 35 cycles was nearly 20 times as that of during C_0, however, the increase was a little lower during early stages of cyclic loading (Table 3). The increased resistance to liquefaction could be attributed due to the denser configuration of soil particles that resulted from reconsolidation after each round of cyclic loading. The difference in $q_{\max}$, CSR and r_u at given number of cycles during subsequent loading levels increased with p'_c (Table 3) and could be attributed to the increased volumetric strains exhibited during the reconsolidation process (Table 2). The pore pressure response at the end of 35 cycles was found to exhibit r_u values of around 0.99 and 0.93 for C_0 and C_4, respectively, implying increased liquefaction resistance.

The excess pore pressure evolution (Δu) under four repeated rounds of cyclic loading is shown in Fig. 5. Excess pore water pressure evolution (Δu) during the subsequent levels of loading showed prominent maximum and minimum Δu within each cycle of loading. This was addressed as transient or oscillatory excess pore water pressure by Zen and Yamazaki [28]. The zone bounded by maximum and minimum Δu widened as the loading progressed from C_1 to C_4. This behavior exhibited the increased liquefaction resistance under the subsequent repeated multilevel cyclic loading. Anbazhagan [1] reported similar findings for soils with higher liquefaction resistance as they exhibited larger and wider oscillatory pore pressure response as compared to soils with lower liquefaction resistance. Seed and Rahman [22] reported that oscillatory response was most common in marine sediments except for non-cohesive sediments of loose to medium density. In the current study, the soil behavior shifted to more liquefaction resistant soil behavior on subsequent levels of cyclic loading.

3.3 *Effective Stress Path Behavior Under Repeated Multilevel Cyclic Loading*

The variations in deviatoric stress (q) and mean effective pressure (p') during the applied repeated cyclic loading were evaluated by following Cambridge soil mechanics group's definition of $p' - q$; where p' and q were evaluated to be $(\sigma'_1 + 2 * \sigma'_3)/3$ and $(\sigma_1 - \sigma_3)$, respectively. Figure 4a illustrates the cyclic effective stress path behavior of Chang dam soil subjected to C_0. The stress path at three initial confining pressures evolved with rapid reduction in p' due to large evolution of r_u subsequently leading to initial liquefaction within 10 cycles of the applied cyclic loading. The stress paths reached the instability line established from isotropically consolidated undrained triaxial compression tests [6] during the second cycle of loading at all the three p'_c.

Figure 6 illustrates the effective stress path response of Chang dam soil under repeated cyclic loading; C_1, C_2, C_3, and C_4. It could be observed that subsequent loading in soil mass exhibited higher mobilization of deviatoric stress, therefore, higher liquefaction resistance. On subsequent loading rounds, the slope of the q_{max} envelope, which coincided with the slope of the instability line during C_0, became steeper. The stress states $(p' - q)$ at the end of 35 cycles of loading were observed to move gradually away from the stress origin indicating significant presence of

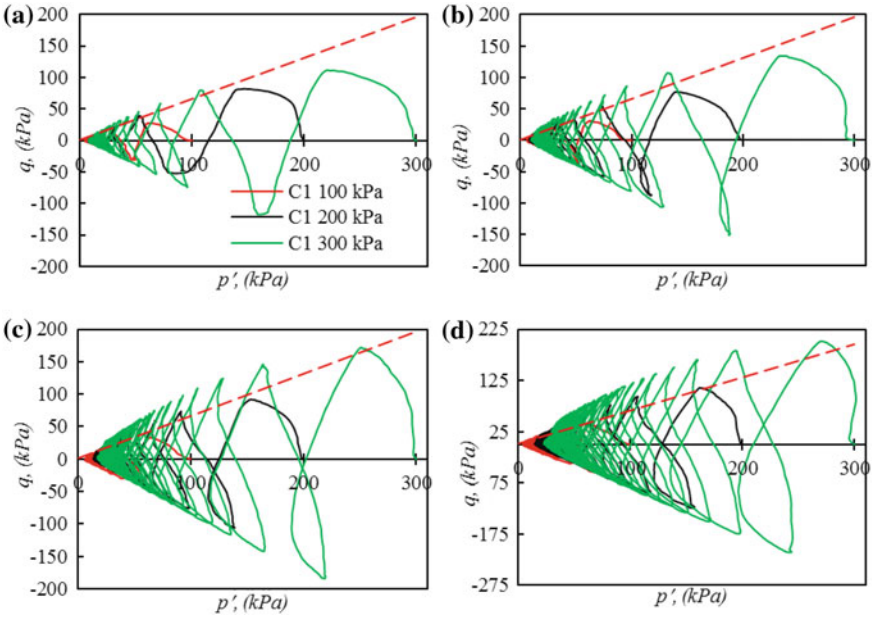

Fig. 6 Evolution of effective stress path under repeated multilevel cyclic loading. **a** C_1, **b** C_2, **c** C_3, **d** C_4

mean effective confining pressure (p') at the end of cyclic loading. Thus, the increase in liquefaction resistance increased with exposure to more levels of cyclic loading, which was further enhanced at higher initial confining pressures (p'_c). This supports the fact that the probability of liquefaction of a soil deposit during a future earthquake is greatly reduced for the soil, which has experienced liquefaction due to a similar magnitude earthquake.

The evolution of effective stress path under initial and repeated cyclic loading revealed strong impact of pre-shearing on the cyclic behavior of soil. The increase in the liquefaction resistance after cyclic pre-shearing was observed to be higher when level of pre-shearing was lower: low γ_{max} and lower r_u [15, 17]. With repeated cyclic shearing, the effective stress path moved away from the origin. The positive effect on the rate of excess pore water pressure development and effective stress path pattern could be helpful in mitigating the liquefaction, provided the initial pre-shear stress levels should remain below critical value and should not induce intolerable residual deformations. The effect of pre-shear repeated cyclic loading is effective only when the soil mass is allowed to reconsolidate after each level of loading.

4 Conclusions

This paper evaluated the reconsolidation and liquefaction behavior of previously liquefied medium dense silty-sand of Chang dam under multilevel cyclic loading. The experiments were conducted under cyclic triaxial conditions and the results were analyzed in the context of reconsolidation volumetric strains, cyclic stress–strain behavior, excess pore water evolution and effective stress path response. In summary, the post-liquefaction reconsolidation and liquefaction behavior under multilevel cyclic loading revealed the followings:

- Chang dam soil inherently has very low liquefaction resistance with excess pore water pressure (Δu) nearly reaching to initial effective confining pressure (p'_c) within 10 cycles of applied dynamic loading. Interestingly, the specimens consolidated to 300 kPa besides 100 kPa and 200 kPa also exhibited liquefaction within 10 cycles indicating very high susceptibility to liquefaction even at greater depths (~30 m).
- During reconsolidation, large volumetric strains as high as 6% were measured leading to reduction in void ratio by 0.052. The volumetric strains were found to increase with the increase in initial effective confining pressure (p'_c) but decreased with the subsequent levels of cyclic loading.
- The peak stress (q_{max}) during the first cycle of first level (C_1) of loading was observed to be lower as compared to the corresponding value of C_0 and could be attributed to the weakening of the soil fabric due to development of excessively high excess pore water pressure during C_0. During subsequent rounds of cyclic loading, the q_{max} was found to be higher than the previous level owing to the increased relative density due to the reconsolidation. The excess pore water pressure during

each cycle of subsequent level of loading was found to be lower as compared to the corresponding value during the previous level of loading.

- Effective stress path response exhibited significant increase in mean effective confining pressure (p') at the end of each level of cyclic loading as compared to previous level of loading. The value of p' was found to be strongly dependent on the initial effective confining pressure (p'_c).
- Cyclic stress ratio (*CSR*) at the end of 35 cycles of fourth repeated loading (C_4) was found to be nearly 20 times as compared to C_0. It showed large increase in liquefaction resistance of Chang dam soil after five levels of each cyclic loading and reconsolidation.

Acknowledgements Financial Support from IIT Gandhinagar is gratefully acknowledged. Any opinions, findings, and conclusions or recommendations expressed in this material are those of authors and do not necessarily reflect the views of IIT Gandhinagar.

References

1. Anbazhagan P (2009) Liquefaction hazard mapping of Bangalore, South India. Disaster Adv 2(2):26–35
2. Amini ZA, Trandafir A (2008) Post-liquefaction shear behavior of Bonneville Silty-Sand. In: Geotechnical Earthquake Engineering and Soil Dynamics, vol IV, pp 1–9
3. Arulanandan K, Sybico J (1992) Post-liquefaction settlement of sand-mechanism and in situ evaluation. Tech Rep NCEER 1(92):239–253
4. Dash HK (2008) Undrained cyclic and monotonic response of sand-silt mixtures. Doctoral dissertation, PhD thesis submitted to Indian Institute of Science, Bangalore in the Faculty of Engineering
5. Finn WD, Bransby PL, Pickering DJ (1970) Effect of strain history on liquefaction of sand. J Soil Mech Found Div 96(SM6)
6. Hussain M, Bhattacharya D, Sachan A (2019) Static liquefaction response of medium dense silty-sand of Chang dam. In: 8th international conference on case histories in geotechnical engineering. Geo-Congress, Philadelphia, USA, March, 24–27, 2019
7. Hamada M, Towhata I, Yasuda S, Isoyama R (1987) Study on permanent ground displacement induced by seismic liquefaction. Comput Geotech 4(4):197–220
8. Ishihara K, Yoshimine M (1992) Evaluation of settlements in sand deposits following liquefaction during earthquakes. Soils Found 32(1):173–188
9. Ishihara K, Okada S (1982) Effects of large preshearing on cyclic behavior of sand. Soils Found 22(3):109–125
10. Kokusho T, Kojima T (2002) Mechanism for postliquefaction water film generation in layered sand. J Geotech Geoenvironmental Eng 128(2):129–137
11. Lade PV (1972) The stress-strain and strength characteristics of cohesionless soils. Thesis Doctoral, University of California, Berkeley
12. Olson SM, Stark TD (2003) Yield strength ratio and liquefaction analysis of slopes and embankments. J Geotech Geoenvironmental Eng 129(8):727–737
13. Olson SM, Stark TD (2002) Liquefied strength ratio from liquefaction flow failure case histories. Can Geotech J 39(3):629–647
14. Oda M, Kawamoto K, Suzuki K, Fujimori H, Sato M (2001) Microstructural interpretation on reliquefaction of saturated granular soils under cyclic loading. J Geotech Geoenvironmental Eng 127(5):416–423

15. Porcino D, Marcianò V, Nicola Ghionna V (2009) Influence of cyclic pre-shearing on undrained behaviour of carbonate sand in simple shear tests. Geomech Geoengin: Int J 4(2):151–161
16. Robertson PK (2009) Evaluation of flow liquefaction and liquefied strength using the cone penetration test. J Geotech Geoenvironmental Eng 136(6):842–853
17. Sriskandakumar S, Wijewickreme D, Byrne PM (2012) Multiple cyclic loading response of loose air-pluviated Fraser River sand. In: Proceedings of the 15th world conference on earthquake engineering. Lisbon, September 24–28, 2012
18. Sitharam TG, Vinod JS, Ravishankar BV (2009) Post-liquefaction undrained monotonic behaviour of sands: experiments and DEM simulations. Géotechnique 59(9):739–749
19. Singh R, Roy D, Jain SK (2005) Analysis of earth dams affected by the 2001 Bhuj earthquake. Eng Geol 80(3–4):282–291
20. Soo Ha I, Ho Park Y, Mo Kim M (2003) Dissipation pattern of excess pore pressure after liquefaction in saturated sand deposits. Transp Res Rec: J Transp Res Board 1821:59–67
21. Scott RF (1986) Solidification and consolidation of a liquefied sand column. Soils Found 26(4):23–31
22. Seed HB, Rahman MS (1978) Wave-induced pore pressure in relation to ocean floor stability of cohesionless soils. Mar Georesour Geotechnol 3(2):123–150
23. Toyota N (1995) Post-cyclic triaxial behaviour of Toyoura sand. In: Proceedings of IS-TOKYO96, vol 1, pp 189–195
24. Vaid YP, Thomas J (1995) Liquefaction and postliquefaction behavior of sand. J Geotech Eng 121(2):163–173
25. Wang S, Luna R, Zhao H (2015) Cyclic and post-cyclic shear behavior of low-plasticity silt with varying clay content. Soil Dyn Earthq Eng 75:112–120
26. Wang S, Luna R, Onyejekwe S (2015) Postliquefaction behavior of low-plasticity silt at various degrees of reconsolidation. Soil Dyn Earthq Eng 75:259–264
27. Youd TL, Hansen CM, Bartlett SF (2002) Revised multilinear regression equations for prediction of lateral spread displacement. J Geotech Geoenvironmental Eng 128(12):1007–1017
28. Zen K, Yamazaki H (1990) Oscillatory pore pressure and liquefaction in seabed induced by ocean waves. Soils Found 30(4):147–161